Oxidative brain damage in Mecp2-mutant murine models of Rett syndrome

Claudio De Felice [a,*,1], Floriana Della Ragione [b,c,1], Cinzia Signorini [d,1], Silvia Leoncini [d,e], Alessandra Pecorelli [d,e], Lucia Ciccoli [d], Francesco Scalabrì [c], Federico Marracino [c], Michele Madonna [c], Giuseppe Belmonte [d], Laura Ricceri [f], Bianca De Filippis [f], Giovanni Laviola [f], Giuseppe Valacchi [g], Thierry Durand [h], Jean-Marie Galano [h], Camille Oger [h], Alexandre Guy [h], Valérie Bultel-Poncé [h], Jacky Guy [i,2], Stefania Filosa [b,c,2], Joussef Hayek [e,2], Maurizio D'Esposito [b,c,**,2]

[a] Neonatal Intensive Care Unit, University Hospital AOUS, Siena, Italy
[b] Institute of Genetics and Biophysics "A. Buzzati-Traverso", Naples, Italy
[c] IRCCS Neuromed, Pozzilli, Italy
[d] Department of Molecular and Developmental Medicine, University of Siena, Siena, Italy
[e] Child Neuropsychiatry Unit, University Hospital AOUS, Siena, Italy
[f] Department of Cell Biology and Neuroscience, ISS, Rome, Italy
[g] Department of Life Sciences and Biotechnologies, University of Ferrara, Ferrara, Italy
[h] Institut des Biomolécules Max Mousseron (IBMM), UMR 5247-CNRS-UM I-UM II-ENSCM, Montpellier, France
[i] Wellcome Trust Centre for Cell Biology, University of Edinburgh, Edinburgh, United Kingdom

ARTICLE INFO

ABSTRACT

Rett syndrome (RTT) is a rare neurodevelopmental disorder affecting almost exclusively females, caused in the overwhelming majority of the cases by loss-of-function mutations in the gene encoding methyl-CpG binding protein 2 (MECP2). High circulating levels of oxidative stress (OS) markers in patients suggest the involvement of OS in the RTT pathogenesis. To investigate the occurrence of oxidative brain damage in Mecp2 mutant mouse models, several OS markers were evaluated in whole brains of Mecp2-null (pre-symptomatic, symptomatic, and rescued) and Mecp2-308 mutated (pre-symptomatic and symptomatic) mice, and compared to those of wild type littermates. Selected OS markers included non-protein-bound iron, isoprostanes (F_2-isoprostanes, F_4-neuroprostanes, F_2-dihomo-isoprostanes) and 4-hydroxy-2-nonenal protein adducts. Our findings indicate that oxidative brain damage 1) occurs in both Mecp2-null (both −/y and stop/y) and Mecp2-308 (both 308/y males and 308/+ females) mouse models of RTT; 2) precedes the onset of symptoms in both Mecp2-null and Mecp2-308 models; and 3) is rescued by Mecp2 brain specific gene reactivation. Our data provide direct evidence of the link between Mecp2 deficiency, oxidative stress and RTT pathology, as demonstrated by the rescue of the brain oxidative homeostasis following brain-specifically Mecp2-reactivated mice. The present study indicates that oxidative brain damage is a previously unrecognized hallmark feature of murine RTT, and suggests that Mecp2 is involved in the protection of the brain from oxidative stress.

Introduction

Rett syndrome (RTT, MIM 312750) is a progressive neurodevelopmental disorder affecting almost exclusively the female gender with a frequency of approximately 1:10,000 live births, and is a leading cause of severe intellectual disability and autistic features (Chahrour and Zoghbi, 2007; Weaving et al., 2005). Other features include stereotypic hand movements, communication dysfunction, seizures, postural hypotonia, tremors, autonomic dysfunction, microcephaly and growth failure (Chahrour and Zoghbi, 2007). The classical clinical picture of the disease (Rett, 1966) is characterized by a period of 6 to 18 months of apparently normal neurodevelopment, followed by an early neurological regression, with a progressive loss of acquired cognitive, social, and motor skills in a typical 4-stage neurological regression pattern (Hagberg, 2002; Neul et al., 2010).

RTT is known to be caused in the overwhelming majority of the cases by sporadic de novo loss-of-function mutations in the X-linked methyl-CpG-binding protein 2 (*MECP2*) gene (Amir et al., 1999) encoding methyl-CpG binding protein 2 (MeCP2), a nuclear protein that binds to methylated CpGs and regulates gene expression (Chahrour et al., 2008; Jones et al., 1998). Different types of mutations within *MECP2* are known to cause RTT, including missense, nonsense, deletions and insertions (Bienvenu and Chelly, 2006).

Despite almost two decades of research into the functions and role of MeCP2, surprisingly little is known about the mechanisms leading from MeCP2 deficiency to disease expression, with many questions still unsolved regarding the role of MeCP2 in the brain and, more generally, during development and in physiopathology (Guy et al., 2011; Zachariah et al., 2012).

Over the last decade, several cellular and mouse models have been developed (Bertulat et al., 2012; Calfa et al., 2011; Cheung et al., 2011; Delepine et al., 2013; Yazdani et al., 2012). Recently, primary fibroblasts from RTT patients highlighted a role of MeCP2 in stabilizing microtubule dynamics, explaining in part the observed dendritic abnormalities found in the absence of functional MeCP2 (Delepine et al., 2013).

Mouse models, in which the *Mecp2* allele has been modified to prevent production of a fully functional Mecp2 protein, have been established. Mice range from *Mecp2*-null mutations to specific point mutations mimicking those observed in humans, phenocopying several motor and cognitive features of RTT patients (Chen et al., 2001; Guy et al., 2001; Moretti et al., 2005, 2006; Picker et al., 2006; Santos et al., 2007; Shahbazian et al., 2002). Although mice cannot model all aspects of the human RTT, certainly they recapitulate many features of the disease and are generally accepted as excellent tools to study MeCP2 function (Ricceri et al., 2008). Although no treatments able to fully arrest or rescue the neurological regression are to date available for the human disease, intriguingly, delayed reintroduction of Mecp2 into fully affected *Mecp2*-null mice is sufficient to rescue RTT-like phenotypes (Guy et al., 2007; Robinson et al., 2012). Restoration of Mecp2 function in astrocytes alone significantly improves the developmental outcome of *Mecp2*-null mice (Lioy et al., 2011). These findings strongly indicate that the RTT phenotype is reversible upon restoration of Mecp2 function. A recent report on the feasibility of a systemic delivery of Mecp2, rescuing behavioral and cellular deficits in female mouse model of RTT strongly supports this point (Garg et al., 2013). In this scenario, microglia was shown to be a major player in the pathophysiology of RTT, thus suggesting that bone marrow transplantation might offer a feasible therapeutic approach for this disorder (Derecki et al., 2012, 2013).

The occurrence of a redox imbalance in RTT has been previously reported both in patients (De Felice et al., 2009, 2011; Durand et al., 2013; Grillo et al., 2013; Leoncini et al., 2011; Pecorelli et al., 2011; Sierra et al., 2001; Signorini et al., 2011) and in an experimental mouse model (Grosser et al., 2012). However, a clear evidence of oxidative damage in the brain, the key organ in this neurodevelopmental disease, is still lacking to date.

Oxidative stress is a condition in which the free radical insult is predominant on the antioxidant defense, with a consequent oxidative-mediated damage of biomolecules known to be relevant in different pathologies (Halliwell and Gutteridge, 2007). To this regard, in the brain, given its high content in lipids, the lipid peroxidation end-products isoprostanes (IsoPs) have a major pathogenetic relevance. IsoPs are a unique series of prostaglandin-like compounds generated, via a free radical-catalyzed mechanism, from a number of different polyunsaturated fatty acids (PUFAs), including arachidonic acid (ARA), eicosapentaenoic acid (EPA), adrenic acid (AdA), and docosahexaenoic acid (DHA). Plasma F_2-IsoPs originating from ARA are considered as an index of generalized lipid peroxidation, whereas the IsoPs originating from DHA are usually termed F_4-NeuroPs due to its main localization in the nervous tissue. F_2-dihomo-IsoPs, deriving from Ada oxidation, have been characterized as potential markers of free radical damage to the myelin in the human brain (Signorini et al., 2013). All types of IsoPs can been evaluated in their esterified form at the cellular site to supply specific information on the lipid cell oxidation, and IsoPs have been extensively investigated in neurological disease (Durand et al., 2013; Singh et al., 2010). At the same time, redox active iron, such as the non-protein-bound iron (NPBI), is considered a trigger of free radical reaction and the relevance of the iron homeostasis in the brain pathologies is well documented (Rouault, 2013; Schroder et al., 2013).

As for isoprostanes, there are also numerous findings supporting the important presence of 4-hydroxy-2-nonenal (4-HNE) protein adducts in many oxidative stress related neurological diseases. For example, increased 4-HNE levels have been observed in the brain tissue from patients with Alzheimer's disease, Pick's disease, Lewy bodies related diseases, amyotrophic lateral sclerosis, Huntington's disease and Parkinson's disease, indicating therefore, a pathophysiological role of this aldehyde and its ability to form protein adducts in several pathologies (Poli et al., 2008). Moreover, a marked increase of 4-HNE was also detectable in the blood of patients with neurodegenerative and neuropsychiatric diseases (Pecorelli et al., 2013; Poli et al., 2008; Valacchi et al., 2014), confirming that this is a reliable marker of oxidative stress not only at the tissue levels, but also at the systemic level.

In the present study we investigated the relationship between oxidative damage and phenotypic expression of RTT, by assessing several oxidative stress (OS) markers in whole brain tissues from different Mecp2 mutant experimental models, as well as in a model of brain specific reactivation of Mecp2.

Materials and methods

Breeding

Mecp2 $-$/y (B6.129P(C) $-Mecp2^{tm1.1Bird}$/J Jax stock number: 003890), *Mecp2*-308 (B6.129S-*Mecp2*^{tm1Hzo}/J Jax stock number: 005439), *Mecp2* stop/y (B6.129P2-*Mecp2*^{tm2Bird}/J Jax stock number: 006849) and NestinCre mice (B6.Cg-Tg(Nest-cre)1Jln/J Jax stock number: 003771) all back crossed to C57BL6/J for at least 12 generations were maintained under standard conditions and in accordance with Home Office regulations and licenses.

Mecp2 mutant hemizygous males and heterozygous females were obtained by mating heterozygous females with wt males. Wild type littermates were used as controls. *Mecp2* stop/y NestinCre males were produced by mating heterozygous *Mecp2* +/stop females with hemizygous NestinCre males.

The animals were sacrificed and the tissues were recovered and stored at $-80\ °C$. The national or institutional guidelines were used for the care and use of animals, and approval for the experiments were obtained from the ethical committees of the Italian Ministry of Health, and the UK Home Office.

Genotyping

Genomic DNA was extracted from ear clips or tail tips of pups. The genotype of the mice was determined by polymerase chain reaction using PCR primers and following the conditions described in the web site of the Jackson Laboratories (USA).

Scoring of symptoms

Mice were scored on a weekly basis for a number of symptoms arising from Mecp2 deficiency as previously reported (Guy et al., 2007). Phenotype severity was expressed as aggregate score.

Blood sampling

Blood was collected in heparinized tubes and all manipulations were carried out within 2 h after sample collection. The blood samples were centrifuged at 2400 g for 15 min at 4 °C and plasma was collected. Butylated hydroxytoluene (BHT) (90 μM) was added to platelet poor plasma as an antioxidant. The resulting plasma samples, strictly hemoglobin-free, were stored at −80 °C until assay. Plasma was used for free F_2-IsoPs, F_4-NeuroPs, and F_2-dihomo-IsoPs determinations.

Brain collection

After transcardial perfusion with saline, brains were removed and bisected on the sagittal plane. Brain hemispheres were immediately frozen in dry ice and stored at −80 °C until assay. At the time of the assays, brain was homogenized (10% W/V) in phosphate-buffered saline (PBS), pH 7.4. Brain homogenate was used for the determination of total (sum of free and esterified) F_2-IsoPs, F_4-NeuroPs, and F_2-dihomo-IsoPs, as well as for NPBI quantification. Brain tissue lysates were also used for 4-HNE-PA adduct determination.

Indirect ImmunoFluorescence (IIF) analysis

Brains were dissected out, fixed in ethanol (60%), acetic acid (10%), and chloroform (30%), and included in paraffin. Paraffin embedded tissue sections of a thickness of 4 μm were deparaffinized in xylene and rehydrated in graded ethanol solutions (100%, 95%, 80% and 70%) for 5 min each.

Sections were rinsed twice in dH$_2$O for 5 min each.

Briefly, antigen retrieval was obtained by incubation with buffer 10 mM citrate pH 6.0, at a temperature sub-boiling for 20 min. Slides were left to cool for 10 min.

After blocking with PBS containing 5% BSA for 60 min, the sections were incubated with the primary antibody (mouse anti-GFAP clone GA5 Millipore 1:200, mouse anti-βIII tubulin isoform clone TU-20 Millipore 1:50; rabbit anti-8 isoProstaglandin F2 alpha Abcam 1:200), overnight at 4 °C.

Incubation in secondary antibody fluorochrome conjugate (goat anti-rabbit Alexa Fluor 488, goat anti-mouse Alexa Fluor 568) diluted 1:100 in antibody dilution buffer was performed for 1 h at room temperature in the dark.

The nuclei were counterstained by incubating the sections for 10 min with 4′,6-diamidino-2-phenylindole (DAPI). Slides were washed with PBS, and mounted with Antifade. Negative controls were generated by omitting the primary antibody. The fluorescence was observed under a microscope Leica AF CTR6500HS (Microsystems).

Western blot analysis

Protein extracts for western blot analysis were obtained from whole brains. Tissues were collected in ice cold PBS, then homogenized in RIPA buffer (20 mM Tris–Cl pH 7.5, 150 mM NaCl, 1% Nonidet P-40, 0.5% sodium deoxycholate, 1 mM EDTA, 0.1% SDS) with Protease Inhibitor Cocktail by Turrax homogenizer. After 20 min of incubation in ice, the homogenate was centrifuged at maximum speed for 20 min at 4 °C, and the supernatant was stored at −80 °C. Protein extracts were run on 10% SDS-PAGE gel with 50 μg protein per lane. Western blot assays were performed with 1:2000 dilution of MeCP2 rabbit polyclonal antibody (Sigma-Aldrich, M9317). β-Actin rabbit polyclonal antibody (Sigma-Aldrich, 1:2500 dilution) was used as loading control. Following washes in PBS–Tween and incubation with specific secondary antibody (goat anti-rabbit horseradish peroxidase-conjugated, Santa Cruz Biotechnology Inc., CA, USA) for 1 h at RT, the membranes were incubated with Supersignal West Pico Chemiluminescent Substrate (Pierce Biotechnology, Rockford, USA). Signals were visualized on Amersham Hyperfilm ECL (GE Healthcare Europe GmbH, Milan, Italy).

Isoprostane and F_4-neuroprostane determinations

All isoprostane and neuroprostane determinations were carried out by gas chromatography/negative ion chemical ionization tandem mass spectrometry (GC/NICI–MS/MS) analysis after solid phase extraction and derivatization steps.

Solid phase extraction and derivatization procedures

Each plasma sample was spiked with tetradeuterated prostaglandin $F_{2\alpha}$ ($PGF_{2\alpha}$-d$_4$) (500 pg in 50 ml of ethanol), as an internal standard. After acidification (2 ml of acidified water, pH 3), the extraction and purification procedures were carried out. It consisted of two solid-phase separation steps: an octadecylsilane (C_{18}) cartridge followed by an aminopropyl (NH$_2$) cartridge (Signorini et al., 2003). Each brain homogenate sample was purified as previously reported (Signorini et al., 2009). Briefly, to an aliquot (1 ml) of brain homogenate aqueous KOH (1 mM, 500 μl) was added. After incubation at 45 °C for 45 min, the pH was adjusted to 3 by adding HCl (1 mM, 500 μl). Each sample was spiked with tetradeuterated prostaglandin $F_{2\alpha}$ ($PGF_2\alpha$-d$_4$) (500 pg in 50 μl of ethanol), as an internal standard, and ethyl acetate (10 ml) was added to extract total lipids by vortex-mixing and centrifugation at 1000 g for 5 min at room temperature. The total lipid extract was applied onto an NH$_2$ cartridge and isoprostanes were eluted.

For both plasma and brain eluted samples, the carboxylic group was derivatized as the pentafluorobenzyl ester, whereas the hydroxyl groups were converted to trimethylsilyl ethers (Signorini et al., 2003).

F_2-isoprostane GC/NICI–MS/MS

The measured ions were the product ions at m/z 299 and m/z 303 derived from the [M − 181]$^-$ precursor ions (m/z 569 and m/z 573) produced from 15-F_{2t}-IsoPs and the tetradeuterated derivative of prostaglandin $F_{2\alpha}$ ($PGF_{2\alpha}$-d$_4$), respectively (Signorini et al., 2003, 2009).

F_4-NeuroPs GC/NICI–MS/MS

Quantification of F_4-NeuroPs was performed by gas chromatography/negative ion chemical ionization tandem mass spectrometry (GC/NICI–MS/MS) according to a new method recently setup in our laboratory (Signorini et al., 2003, 2009). The measured ions were the product ions at m/z 323 and m/z 303 derived from the [M − 181]$^-$ precursor ions (m/z 593 and m/z 573) produced from oxidized DHA and the tetradeuterated derivative of $PGF_{2\alpha}$, respectively.

F_2-dihomo-IsoPs GC/NICI–MS/MS

For F_2-dihomo-IsoPs, the measured ions are the product ions at m/z 327 and m/z 303 derived from the [M − 181]$^-$ precursor ions (m/z 597 and m/z 573) produced from the derivatized ent-7(RS)-F_{2t}-dihomo-IsoP and 17-F_{2t}-dihomo-IsoP, and the $PGF_{2\alpha}$-d$_4$, respectively (De Felice et al., 2011).

Non-protein-bound-iron determination

NPBI is a pro-oxidant factor, associated with hypoxia, hemoglobin oxidation and subsequent heme iron release (Ciccoli et al., 2008). Non-protein-bound-iron was determined as deferoxamine (DFO)–chelatable free iron (DFO–iron complex, ferrioxamine). DFO 25 μM was added to the brain homogenate. The homogenate was ultrafiltered in centrifugal filters with a 30-kDa molecular weight cut-off and the DFO excess removed by silica column chromatography. The DFO–iron complex was determined by high-performance liquid chromatography at the detection wavelength of 229 nm (Signorini et al., 2009).

4-HNE protein adducts

4-HNE PAs are markers of protein oxidation due to aldehyde binding from lipid peroxidation sources (Signorini et al., 2013). Brain 4-HNE protein adducts were determined by western blot technique. Brain tissue proteins (30 μg protein, as determined by using Bio-Rad protein assay; BioRad, Hercules, CA, USA) were resolved on 4–20% SDS-PAGE gels (Lonza Group Ltd., Switzerland) and transferred onto a hybond ECL nitrocellulose membrane (GE Healthcare Europe GmbH, Milan, Italy). After blocking in 3% non-fat milk (Bio-Rad, Hercules, CA, USA), the membranes were incubated overnight at 4 °C with goat polyclonal anti 4-HNE adduct antibody (cod. AB5605; Millipore Corporation, Billerica, MA, USA). Following washes in TBS–Tween and incubation with specific secondary antibody (mouse anti-goat horseradish peroxidase-conjugated, Santa Cruz Biotechnology Inc., CA, USA) for 1 h at RT, the membranes were incubated with ECL reagents (Bio-Rad, Hercules, CA, USA) for 1 min. The bands were visualized by autoradiography. Quantification of the relevant bands was performed by digitally scanning the Amersham Hyperfilm ECL (GE Healthcare Europe GmbH, Milan, Italy) and measuring immunoblotting image densities with ImageJ software.

Statistical analysis

Results were expressed as medians with inter-quartile ranges, or means ± SD. Differences between groups were evaluated by the non-parametric Mann–Whitney rank sum test, Wilcoxon rank test, or Kruskal–Wallis test analysis of variance (ANOVA), as appropriate. Associations between variables were tested by univariate regression analysis. Multiple of medians (*MoMs*) for the brain OS markers were used to account for the possible effect for potential sources of variation including inter- and intra-group differences in strain, age, diet or breeding. The MedCalc ver. 12.0 statistical software package (MedCalc. Software, Mariakerke, Belgium) was used for data analysis. A two-tailed $P < 0.05$ was considered to indicate statistical significance.

Results

The elevated concentrations of F_2-isoprostanes (F_2-IsoPs) in plasma of symptomatic *Mecp2* −/y (median age 9 weeks) and hemizygous *Mecp2* 308/y mutated (median age 32 weeks) mice compared with wild type (wt) indicate the presence of a systemic OS status in the symptomatic phase of the disease (Figs. 1A–B), thus suggesting that these strains constitute reliable RTT animal models to further investigate the link between OS and Mecp2 deficiency.

In order to evaluate whether the oxidative damage observed in this peripheral body fluid is actually associated with oxidative damage in the brain, likely the main target organ of RTT given the major neurological dysfunctions in the patients, the following OS markers, in additions to F_2-IsoPs were evaluated in whole brain from *Mecp2* −/y 7 to 9 weeks symptomatic null mice (median age 9 weeks; mean aggregate score, M ± SD, 4.5 ± 0.43), and compared to age-matched wt littermates: non-protein-bound iron (NPBI), F_2-dihomo-isoprostanes (F_2-dihomo-IsoPs), F_4-neuroprostanes (F_4-NeuroPs) and 4-hydroxy-2-nonenal protein adducts (4-HNE PAs). The severity of the Mecp2-null phenotype
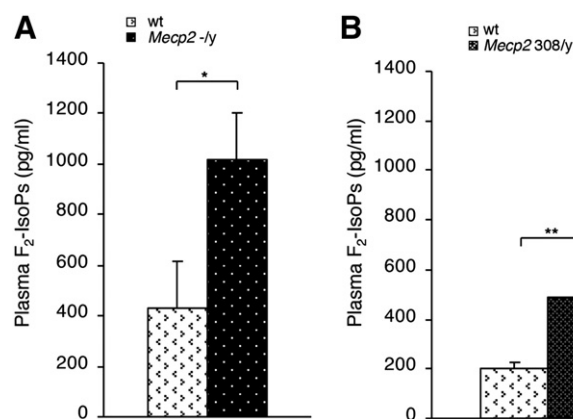

Fig. 1. Oxidative stress in plasma of two murine models of Rett syndrome. Plasma levels of F_2-IsoPs are significantly increased in symptomatic *Mecp2* −/y mice (N = 16, median age, M ± SD, age 9 ± 1.25 weeks) vs. matched wt littermates (N = 15, median age 9 ± 1.2 weeks) (A) and in symptomatic *Mecp2* 308/y (N = 9, median age 32 ± 11 weeks) vs. matched wt littermates (N = 10, median age 32 ± 11 weeks) (B). Data are expressed as medians (columns) and semi-interquartile range (bars). *$P < 0.05$; **$P < 0.01$.

was quantified using a simple phenotypic scoring method (Guy et al., 2007), which assesses a number of RTT like features seen in *Mecp2* mutant mice. Significantly elevated NPBI, F_2-IsoP, and F_4-NeuroP levels were evident in the brain of symptomatic null mice as compared to wt, thus demonstrating the occurrence of brain oxidative damage in the symptomatic phase of the disease (Figs. 2A–C).

These data indicate that the oxidative damage is mainly the consequence of the peroxidation of arachidonic acid (ARA) and docosahexaenoic acid (DHA), i.e., fatty acid precursors of F_2-IsoPs and F_4-NeuroPs, respectively, as triggered by NPBI as pro-oxidant factor. On the other hand, no significant changes for F_2-dihomo-IsoPs or 4-HNE PAs were detectable in this model at this disease stage (Figs. 2D–E; Supplementary Fig. 1A).

To better evaluate the cellular origin of the OS alteration, an immunohistochemical analysis with a specific F_2-IsoP antibody was performed. The assay revealed a strong increase in F_2-IsoPs in βIII tubulin positive cells (neurons, Fig. 3A) but not in glial fibrillary acidic protein (GFAP) positive cells (astroglia, Fig. 3B) of *Mecp2* −/y mice compared to wt, thus indicating the presence of an oxidative damage in neuronal more than in astroglial cells.

Significant inverse relationships of F_4-NeuroPs with brain weight and body weight (Figs. 4A–B) were evidenced, suggesting an involvement of the DHA-derived peroxidation products in the pathogenesis of microcephaly and somatic growth deficiency in the *Mecp2* −/y mouse model of RTT.

In order to evaluate the timing of the oxidative brain damage, we subsequently tested the same OS markers in whole brains from *Mecp2* −/y 5 weeks pre-symptomatic null mice (median age 5 weeks; mean aggregate score 0.25 ± 0.25). As with the symptomatic null animals, brains of pre-symptomatic null mice also showed significantly increased NPBI, F_2-IsoP, and F_4-NeuroP tissue levels compared with wt, thus indicating that the oxidative brain damage, unlike other epiphenomena of the disease, precedes the onset of overt behavioral abnormalities (Figs. 5A–C). On the contrary, as observed in symptomatic mice, no statistical differences for F_2-dihomo-IsoPs or 4-HNE PAs were observed (Figs. 5D–E; Supplementary Fig. 1B).

These data were confirmed by OS marker analysis in an independent strain, in which the endogenous *Mecp2* allele is silenced by a targeted stop cassette (*Mecp2* stop/y) (Guy et al., 2007). *Mecp2* stop/y mice are phenotypically equivalent to *Mecp2* −/y animals and the observed residual expression of Mecp2 of around 2.5% compared with wt levels is not correlated with the severity of symptom progression (Robinson et al., 2012). Altered concentrations of NPBI, F_2-IsoPs, and F_4-NeuroPs are significantly detected in the brain at the pre-symptomatic stage
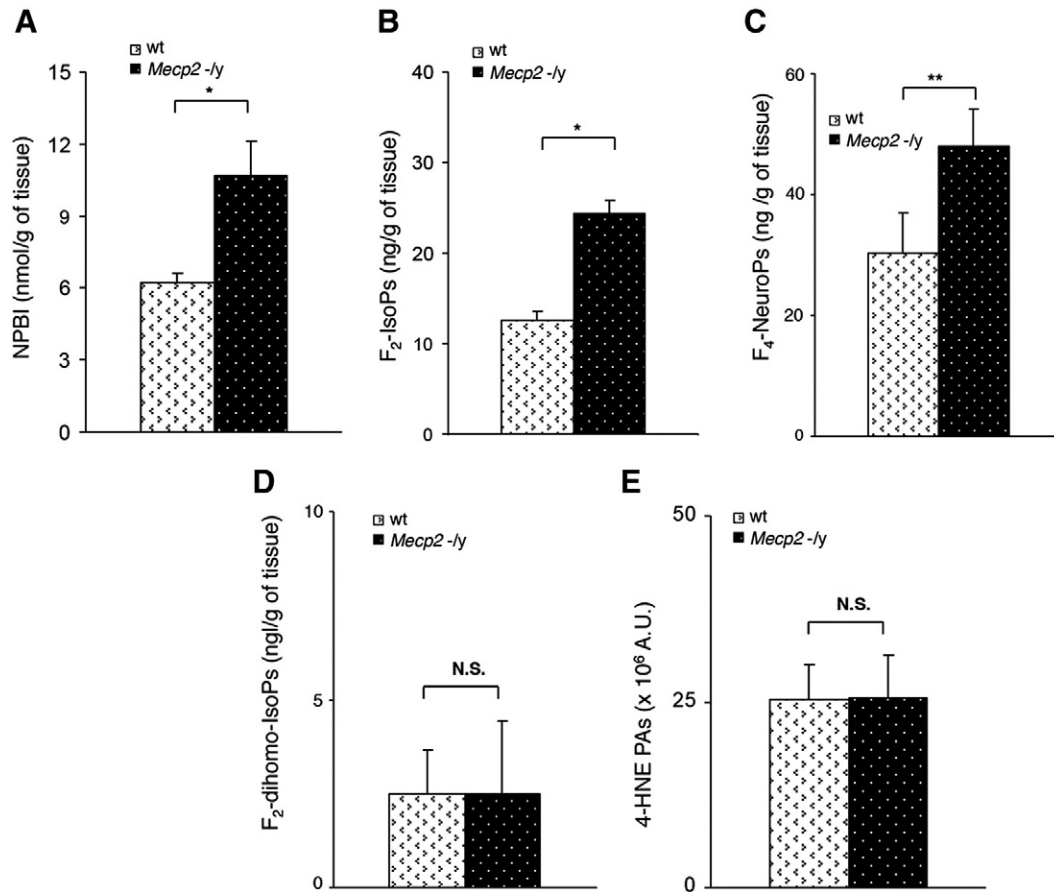
Fig. 2. Evidence of oxidative brain damage in symptomatic *Mecp2* −/y mice (N = 16, median age 9 weeks). Significant increased levels of NPBI (A), F_2-IsoPs (B), and F_4-NeuroPs (C) vs. matched wt littermates (N = 15, mean age 9 ± 1.2 weeks) are observed in whole brain tissue, whereas no significant changes in F_2-dihomo-IsoPs (D), and 4-HNE PAs (E) are detected. Data are expressed as medians (columns) and semi-interquartile range (bars). *$P < 0.05$; **$P < 0.01$. N.S.: no significant differences ($P > 0.05$).

(median age 5 weeks; mean aggregate score 0.25 ± 0.42) (Supplementary Figs. 2A–C), whereas no statistical differences were detectable regarding F_2-dihomo-IsoPs or 4-HNE PAs (Supplementary Figs. 2D–E).

We then evaluated OS alterations in a different RTT mouse model (Shahbazian et al., 2002), with a truncating mutation (*Mecp2*-308). In this specific RTT model, males show a much milder phenotype than human males with RTT-causing mutations, and heterozygous females

also display a milder phenotype than that of RTT girls. These mutant mice live longer and are therefore easier to study as compared to the *Mecp2*-null models.

Therefore, OS markers were tested in the brain tissue of symptomatic *Mecp2* 308/y and *Mecp2* 308/x mice. *Mecp2* 308/y (median age 32 weeks) showed significant increase in NPBI, F_2-IsoPs, F_4-NeuroPs, and 4-HNE PAs as compared to wt mice (Figs. 6A–C, E; Supplementary
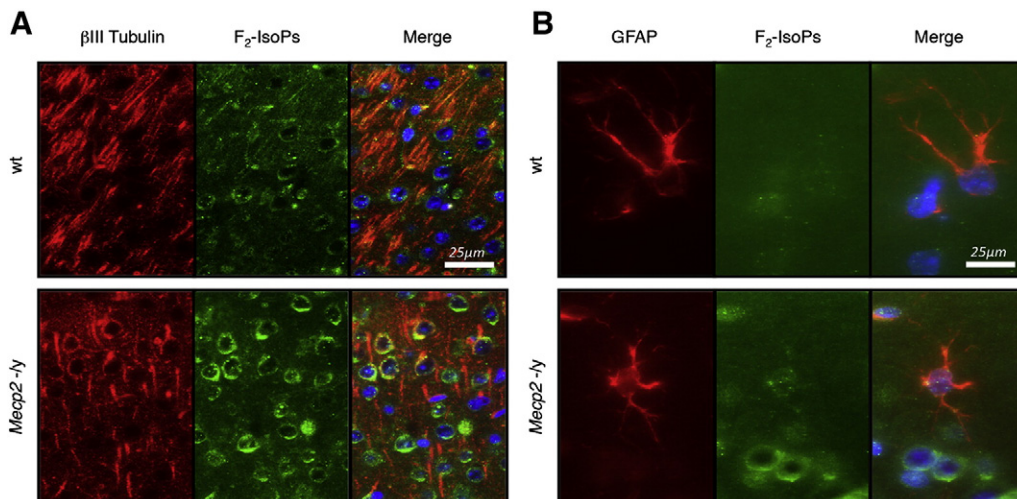

Fig. 3. Double immunofluorescence in the brains of symptomatic *Mecp2* −/y and matched wt littermates at 9 weeks, for F_2-IsoPs (green)/βIII tubulin (red) (A) and for F_2-IsoPs (green)/ GFAP (red) (B). In the merge image the nuclei were identified by counterstaining with the nuclear marker DAPI (blue).
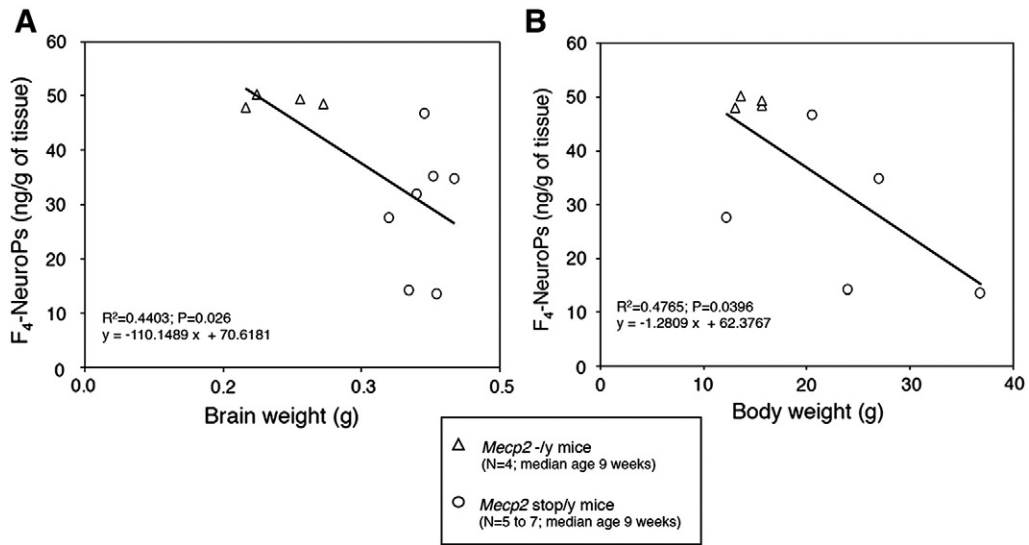
Fig. 4. Inverse linear relationship of brain F_4-NeuroPs vs. brain weight in symptomatic *Mecp2* −/y mice (A) and of brain F_4-NeuroPs vs. body weight in symptomatic *Mecp2* −/y mice (B).

Fig. 1C), thus confirming the relationship between the symptomatic phase of the disease and the fatty acid peroxidation leading to lipid and protein damage. On the other hand, no statistical difference for F_2-dihomo-IsoPs was detectable (Fig. 6D).

Interestingly, heterozygous 308 mutated females (*Mecp2* 308/x), which exhibit a milder form of the disease with a delayed onset of the

behavioral manifestations (median age 54 weeks), showed biochemical signs of oxidative brain damage limited to F_2-IsoPs, and F_4-NeuroPs (Figs. 7B–C), whereas no statistical differences were observed for NPBI, F_2-dihomo-IsoPs, or 4-HNE PAs (Figs. 7A, D–E; Supplementary Fig. 1D).

Likewise, brain oxidative damage precedes the symptomatic phase also in the *Mecp2* 308/x mice, given that presymptomatic animals
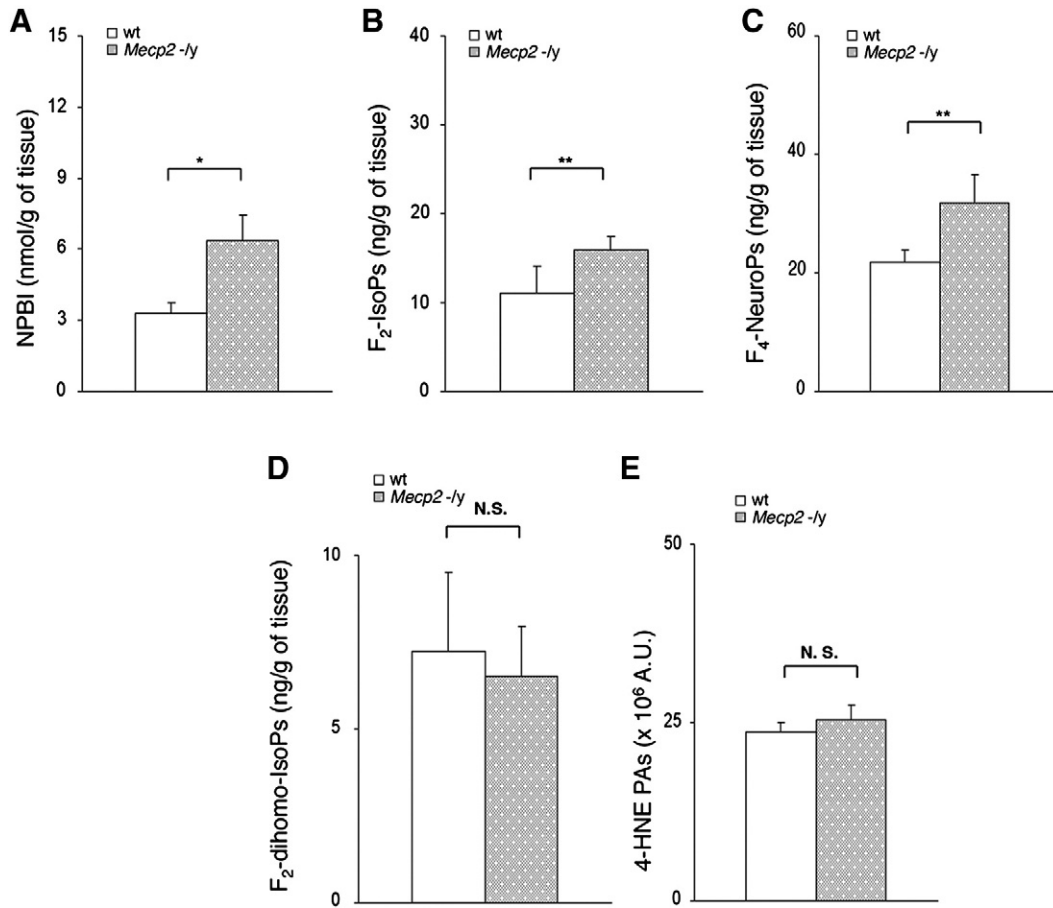

Fig. 5. Evidence of oxidative brain damage in pre-symptomatic *Mecp2* −/y mice vs. matched wt littermates with significant increase of NPBI (A), F_2-IsoP (B), and F_4-NeuroP (C) levels (N = 13, median age 5 weeks). No significant changes for F_2-dihomo-IsoPs (D), and 4-HNE PAs (E) are observed. Data are expressed as medians (columns) and semi-interquartile range (bars). *P < 0.05; **P < 0.01. N.S.: no significant differences (P > 0.05).
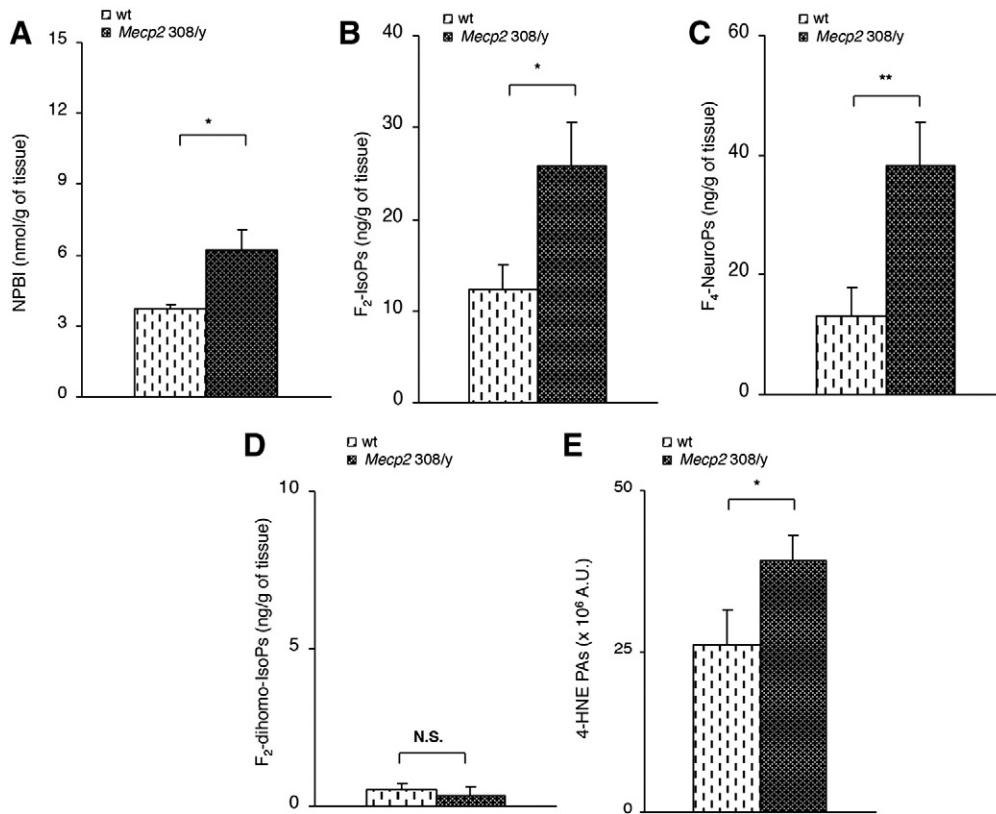
Fig. 6. Evidence of oxidative brain damage in symptomatic hemizygous male *Mecp2*-308 mutated mice vs. matched wt littermates (N = 9, median age 32 weeks) showing significant increase of the assessed OS markers (A–C, E), with the single exception of F_2-dihomo-IsoPs (D). Data are expressed as medians (columns) and semi-interquartile range (bars). $^*P < 0.05$; $^{**}P < 0.01$. N.S.: no significant differences ($P > 0.05$).

(median age 22 weeks) show a significant increase in NPBI, F_2-IsoPs, and F_4-NeuroPs (Figs. 8A–C). In contrast, no significant differences for F_2-dihomo-IsoPs, or 4-HNE PAs were observed between mutant mice and their wt counterparts (Figs. 8D–E).

In order to compare the entity of the different oxidative events in the different *Mecp2* mutant mouse models, the levels of each marker were expressed as a function of the median levels in the age-matched wt controls (multiple of medians of the wt, MoMs) (Supplementary Figs. 3A–E). Besides the need to level off the methodological variability, MoMs were used to account for potential confounders including inter- and intra-group differences in strain, age, diet or breeding. Normalized F_2-IsoP levels were found to be significantly lower in the symptomatic *Mecp2* 308/x and in the presymptomatic *Mecp2* −/y-null mice, thus indicating that brain ARA peroxidation is relatively lower in these models. Symptomatic *Mecp2* 308/y and *Mecp2* stop/y show relatively higher brain levels of 4-HNE PAs, thus indicating that the oxidative protein damage consequent to aldehyde binding is increased in this murine models of the disease.

When comparing the differences between relative OS marker levels in the different mouse models, a trend just at the borders of the statistical significance was observed for F_4-NeuroPs (ANOVA, $P = 0.0587$), whereas no significant differences were detectable for NPBI and F_2-dihomo-IsoPs (Kruskal Wallis ANOVA, $P = 0.2325$ and, $P = 0.1380$, respectively).

No significant relationships between the entity of the brain oxidative damage (as expressed as MoMs for the age-matched wt control population) and the clinical phenotype severity, as expressed as aggregate score (Guy et al., 2007), were observed ($r \leq 0.3499$; $P \leq 0.2010$, data not shown).

In order to further test a potential cause–effect relationship between oxidative brain damage and Mecp2 loss-of-function, brain levels of OS markers were evaluated in brain specific Mecp2 rescued mice.

Specifically, the endogenous *Mecp2* allele silenced by a targeted stop cassette (*Mecp2* stop/y) was activated specifically in the brain during embryogenesis by expressing the Cre recombinase under the control of Nestin promoter (*Mecp2* stop/y NestinCre mice) (Tronche et al., 1999). As expected (Robinson et al., 2012), a variable residual expression of the Mecp2 protein was observed in the brain tissues of the symptomatic *Mecp2* stop/y (mean age 17 weeks; median aggregate score 6.5 ± 0.7), whereas a normal or near to normal Mecp2 expression was detectable in the brain of rescued *Mecp2* stop/y NestinCre animals (mean age 17 weeks; median aggregate score 0) (Fig. 9A).

Symptomatic *Mecp2* stop/y mice, like the *Mecp2* −/y mice, showed oxidative damage in the brain, with NPBI, F_2-IsoP, and F_4-NeuroP levels being significantly elevated as compared to those of age-matched wt expressing Cre recombinase (wt-Cre) littermates, whereas no statistical differences were observed for F_2-dihomo-IsoPs and 4-HNE PAs (Fig. 9B and Supplementary Fig. 3). On the other hand, rescued stop/y mice showed levels of brain OS comparable to those of age-matched wt littermates (Fig. 9B; Supplementary Fig. 1E), thus indicating a full rescue of the brain OS damage following brain specific *Mecp2* gene reactivation, and demonstrating that the altered redox homeostasis at the brain level in this RTT murine model can be fully reversed following restoration of the Mecp2 function.

Discussion

OS has been widely implicated in several pathological conditions including neurological disease (Ferguson, 2010; Halliwell and Gutteridge, 2007; Praticò, 2010). Lipid peroxidation, a critical component of OS, is a process well known to induce oxidative damage to key cellular components, implicated in several diseases. In particular, free radicals and specifically reactive oxygen species (ROS) are able to attack polyunsaturated fatty acids (PUFAs) of cell membranes, thus generating the
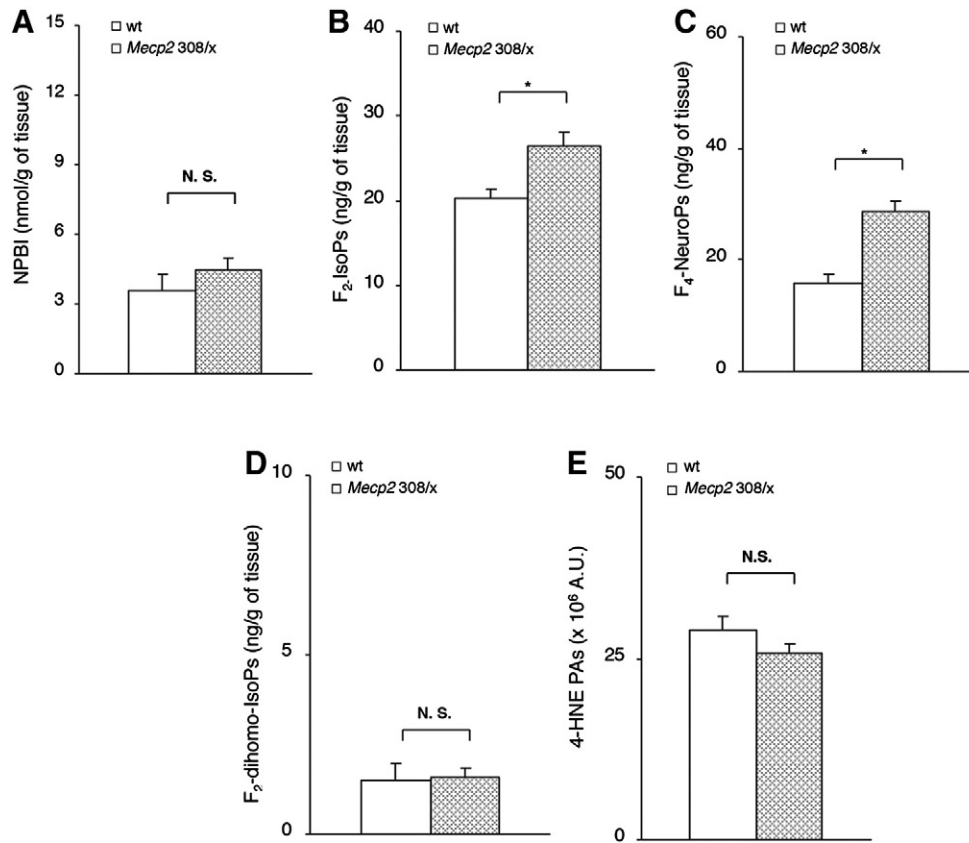
Fig. 7. Evidence of oxidative brain damage in symptomatic heterozygous female *Mecp2*-308 mutated mice vs. matched wt littermates (N = 5, median age 54 weeks) showing significant increase of F_2-IsoPs (B), and F_4-NeuroPs (C). No significant changes in NPBI (A), F_2-dihomo-IsoPs (D), and 4-HNE PAs (E) are observed. Data are expressed as medians (columns) and semi-interquartile range (bars). *$P < 0.01$. N.S.: no significant differences ($P > 0.05$).

prostaglandin-like end-products IsoPs, along with a family of α,β-unsaturated reactive aldehydes, such as 4-HNE.

Isoprostanes are considered as the gold standard for the OS in vivo evaluation (Galano et al., 2013; Signorini et al., 2013). Specifically, F_2-IsoPs are the oxidation end-products of ARA, a polyunsaturated fatty acid, abundant in both brain gray and white matter, F_4-NeuroPs are the end-products of DHA, abundant in neuronal membranes, whereas F_2-dihomo-IsoPs are known to derive from oxidation of AdA (De Felice et al., 2011), a fatty acid abundant in white matter, specifically myelin and can be considered a marker of white matter oxidative damage (Supplementary Fig. 4).

Our data, obtained in established mouse models of Rett syndrome, appear to be in line with the emerging view that a lipid abnormality may be key to the pathogenesis of the Rett syndrome (Buchovecky et al., 2013; De Felice et al., 2013; Nagy and Ackerman, 2013; Sticozzi et al., 2013). Of course, it should always be kept in mind that experimental models for a disease unavoidably carry intrinsic limitations related to inter-species differences with the mimicked human pathology. To this regard, a puzzling discrepancy with the behavior of the OS markers in blood samples from RTT patients is represented by the lack of changes in F_2-dihomo-IsoP levels in the tested RTT mouse models (data not shown), which is in good agreement with the presence of increased level of F_2-IsoPs in neurons but not in astroglia (Fig. 3), but is in contrast with the marked increase in F_2-dihomo-IsoPs previously documented in plasma samples from patients at an early stage of the disease (De Felice et al., 2011).

Nonetheless, the data presented here point out to several interesting considerations:

i) alterations of the redox balance have been confirmed in murine models of RTT. More importantly, imbalances of OS "gold standard" markers are well evident especially in neurons;

ii) our findings indicate that an OS-driven brain damage occurs in two different mouse models of RTT: the *Mecp2*-null and *Mecp2*-308 animals. Thus, our findings further strengthen the above reported observations, having extended our investigation on OS markers to murine RTT models in which Mecp2 is hypofunctional, rather than limiting our studies to *Mecp2*-null mice in which the Mecp2 protein is totally absent (Katz et al., 2012);

iii) brain oxidative damage precedes the clinical manifestations by several weeks in *Mecp2* −/y, stop/y and Mecp2-308/x models, where we detected a significant brain redox alteration prior to symptoms onset. These data are consistent with a close relationship between Mecp2 deficiency and development of RTT, and indicate the existence of a phase of the disease in which biochemical signs of enhanced OS are present in the brain, well before the clinical signs of the pathology, although some clinical evidence suggests that the disease could start at birth or even prenatally (Leonard and Bower, 1998). Notably, prior experimental data obtained with a mouse model carrying *Mecp2* T158A mutation suggest that the underlying deficits in neural activity precede the establishment of behavioral symptoms (Goffin et al., 2012). Furthermore, in vitro electrophysiological studies showed reduced cortical excitability in *Mecp2* −/y mice even at 2–3 weeks of age, that is well before the onset of neurological symptoms (Dani et al., 2005);

iv) in a translational perspective, these findings would strongly suggest that neurology of RTT girls may be abnormal long before the onset of clinical signs, in line with several clinical (Burford et al., 2003; Einspieler et al., 2005a,b; Marschik et al., 2011; Temudo et al., 2007) and preclinical evidence (De Filippis et al., 2010; Picker et al., 2006);
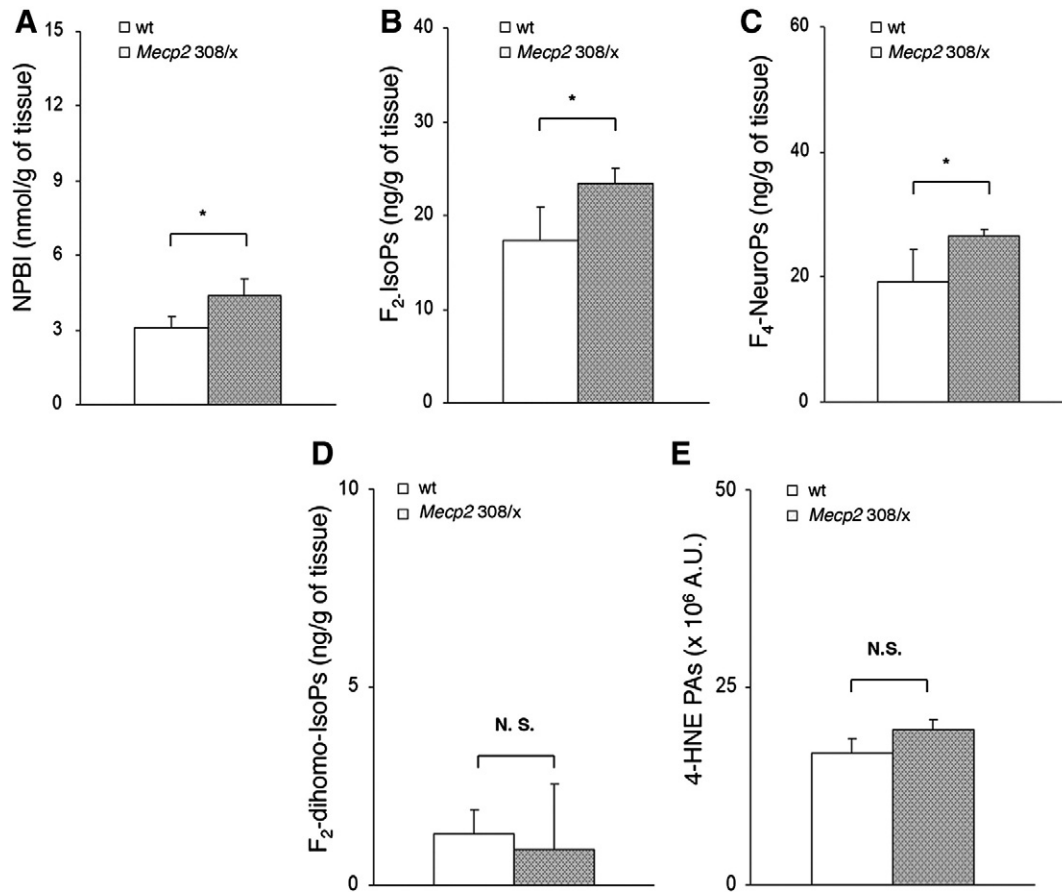
Fig. 8. Evidence of oxidative brain damage in pre-symptomatic heterozygous female *Mecp2*-308 mutated mice showing significant increase of NPBI (A), F_2-IsoPs (B), and F_4-NeuroPs (C) vs. matched wt littermates (N = 3, median age 22 weeks). No significant changes in F_2-dihomo-IsoPs (D), and 4-HNE PAs (E) are observed. Data are expressed as medians (columns) and semi-interquartile range (bars). *$P = 0.0339$. N.S.: no significant differences ($P > 0.05$).

v) the correction of Mecp2 deficient genotype in the rescued *Mecp2* stop/y NestinCre animals, re-establish the correct level of IsoPs. With this experiment we can affirm that the OS imbalance is a reversible phenomenon, which may be corrected by the re-introduction of a functional MeCP2. Moreover, the re-expression of Mecp2 in a Nestin-driven manner strongly suggests that the brain OS imbalance is due to a neural specific impairment of Mecp2 function, although the underlying molecular mechanism is still obscure.

In fact, the occurrence of alterations in OS brain markers, here evidenced when the *Mecp2* gene is knocked out/silenced or mutated, does not necessarily mean that redox control could be a new, direct, function for the Mecp2 protein; our data do only provide clear evidence that Mecp2 deficiency is associated with a brain redox abnormality, thus indicating that oxidative brain damage is a previously unrecognized hallmark feature of murine RTT, and suggesting that Mecp2 is likely involved in the protection of the brain from OS.

Given that a loss of Mecp2 likely leads to the dysregulation of thousands of genes (Chahrour et al., 2008), with all the complex downstream consequences of this, it is not possible, to date, to relate any specific phenotypic features to the increased OS marker levels in the brain and/or plasma of the affected animals. At the same time, it is undeniable that RTT patients and *Mecp2* mutant animal models are facing remarkable breathing challenges, exemplified by recurrent apneas and breath-holds (De Felice et al., 2010; Ramirez et al., 2013), which ultimately lead to a clinical phenotype defined not only by complex genetic causes (Grillo et al., 2013), but also by a series of interacting mechanisms involving a variety of compensatory, synaptic and

neuromodulatory alterations, as well as disturbed homeostasis and OS (Grosser et al., 2012; Ramirez et al., 2013). Since several receptors and ion-channels are known to be redox-modulated (Poli et al., 2008; Sticozzi et al., 2013), it is possible that the mitochondrial (Grosser et al., 2012) and redox changes (De Felice et al., 2009; Grosser et al., 2012) evidenced in patients and animal models could contribute to the hyperexcitability and diminished synaptic plasticity in MeCP2 deficiency.

The key role of OS mechanisms in determining some of the characteristic neurological features in RTT appears to be also confirmed by the recent report on reduction in neuronal hyperexcitability, improvement in synaptic short-term plasticity, and restoration of synaptic long-term potentiation in a Mecp2 null mouse model of the disease following the incubation of hippocampal slices with a free radical scavenger vitamin E derivative compound (Janc and Muller, 2014).

It is important to underline that biochemical signs of brain oxidative damage predate the onset of symptoms, including the respiratory features, in the examined mutant mice. Although human and experimental evidence indicate that Obstructive Sleep Apnea Hypopnea Syndrome and intermittent hypoxia can be associated with enhanced OS, conflicting reports exist (De Felice et al., in press and references therein). However, the relationships between apneas/upper airways obstruction/intermittent hypoxia and OS status in RTT patients appear to be limited to the generation of a pro-oxidant status, as indicated by a reported link between intraerythrocyte-NPBI, but not F_2-IsoPs, and apneas (De Felice et al., in press). Therefore, it becomes clear that mechanisms other than apneas/intermittent hypoxia should be the major sources of enhanced OS in human RTT and, by inference, mouse models of the disease.
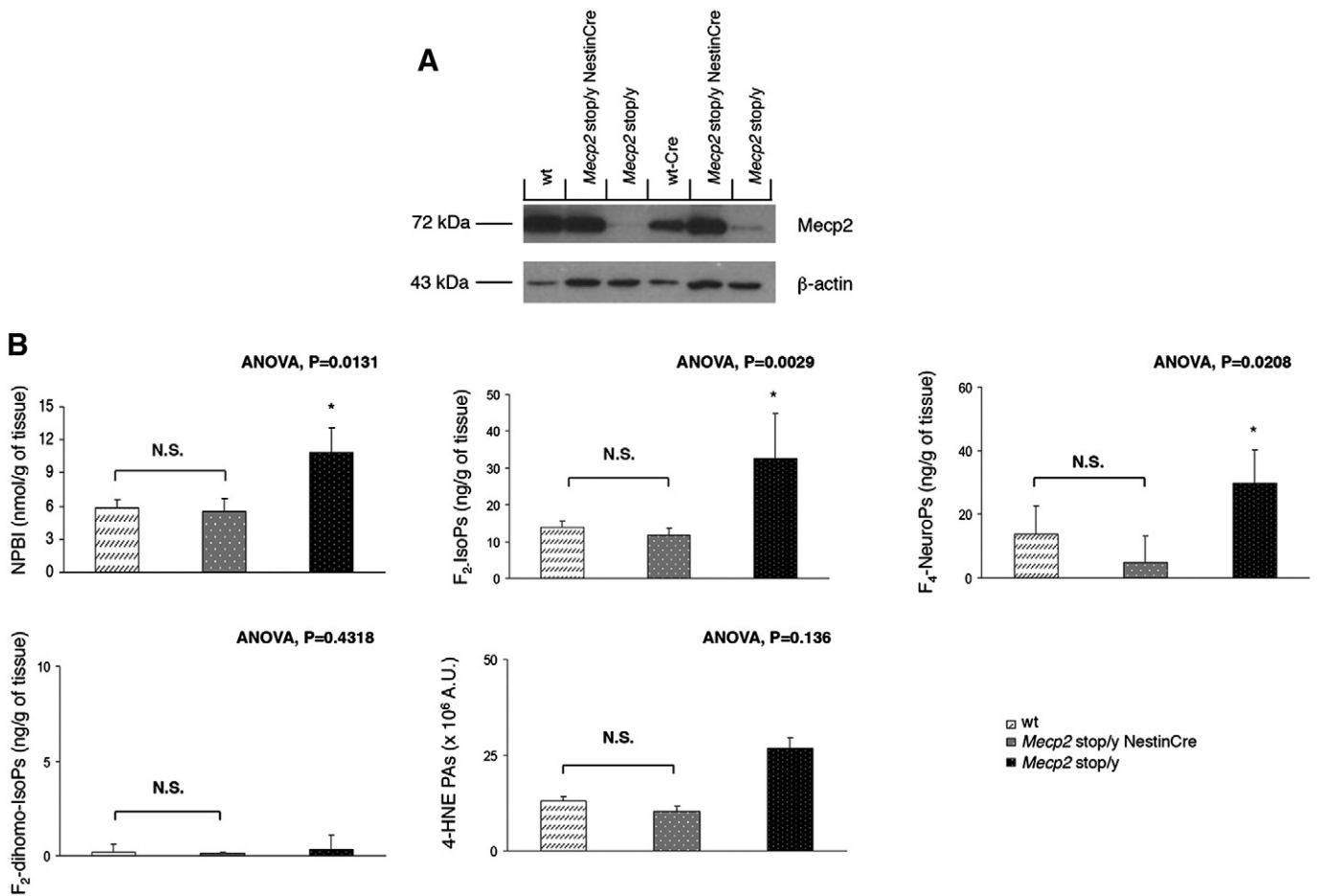
Fig. 9. Rescue of oxidative brain damage in Mecp2 stop/y NestinCre mice. Western blot analysis of Mecp2 protein in the brains of wt, wt-Cre, Mecp2 stop/y, and Mecp2 stop/y NestinCre mice. β-Actin was used as loading control (A). Analysis of NPBI, F_2-IsoPs, F_4-NeuroPs, F_2-dihomo-IsoPs and 4-HNE PAs in the brains of wt-Cre (N = 5, median age 17 weeks), Mecp2 stop/y (N = 2, median age 17 weeks), and Mecp2 stop/y NestinCre (N = 6, median age 17 weeks) mice (B). OS markers are expressed as medians (columns) and semi-interquartile range (bars). ANOVA: Kruskal–Wallis analysis of variance. *$P < 0.05$. N.S.: no statistically significant differences ($P > 0.05$).

Taken as a whole, the oxidative hypothesis of RTT (De Felice et al., 2012b) would seem to explain several intriguing features of the human disease. For instance, the risk of OS-driven brain damage may represent one of the possible reasons why MeCP2 activity must be finely tuned and tightly regulated, including embryonal microRNA control (Han et al., 2013). In addition, the occurrence of biochemical signs of oxidative brain damage preceding the neurological symptoms may explain the inconsistency of the apparently normal developmental phase (i.e., latency period) before clinical onset in the RTT patients. Finally, the previously unrecognized key role of Mecp2 in the regulation of redox homeostasis could explain the potential reversibility of the disease following functional restoration of the Mecp2 protein.

Taken together, our data suggest the existence of a window in which an early OS-modulating therapy could reduce/limit phenotype severity. As there are no currently proven effective pharmacological therapies for human RTT that can either halt progression or reverse the neurological and cognitive abnormalities, although many strategies are ongoing (Panayotis et al., 2011) our findings could pave the way for an early OS-modulating intervention during the preclinical window in RTT. This concept is supported by a previous pilot study in RTT patients at an early stage of the disease using ω-3 PUFAs (De Felice et al., 2012a).

Supplementary data to this article can be found online at http://dx.doi.org/10.1016/j.nbd.2014.04.006.

Author contributions

Concept: CDF, CS, SL, MDE, SF, and JH.

Experimental design: CDF, CS, SL, MDE, FDR, SF, and JH.

Mecp2-null mice breeding and sample collection: JG, SF, FDR, FS, MDE, FM, and MM.

Mecp2-308 truncated mice breeding and sample collection: LR, BDF, and GL.

Sample (brain and blood) preparation: JG, CS, SL, AP, FS, FM, and MM.

Isoprostane and neuroprostane assays: CS and LC.

NPBI assays: SL and LC.

4-HNE-PA assays: AP, LC, and GV.

Isoprostane synthesis: TD, CO, JMG, AG, and VBP.

Double fluorescence immunostaining: GB, AP, CS, and GV.

Data analysis: CDF, CS, SL, FDR, and BDF.

Data interpretation: All the Authors.

Manuscript drafting: all the authors.

Approval: all the authors.

Conflict of interest

The authors have declared that no conflict of interest exists.

References

Amir, R.E., Van den Veyver, I.B., Wan, M., Tran, C.Q., Francke, U., Zoghbi, H.Y., 1999. Rett syndrome is caused by mutations in X-linked MECP2, encoding methyl-CpG-binding protein 2. Nat. Genet. 23, 185–188.

Bertulat, B., De Bonis, M.L., Della Ragione, F., Lehmkuhl, A., Milden, M., Storm, C., Jost, K.L., Scala, S., Hendrich, B., D'Esposito, M., Cardoso, M.C., 2012. MeCP2 dependent heterochromatin reorganization during neural differentiation of a novel Mecp2-deficient embryonic stem cell reporter line. PLoS One 7, e47848.

Bienvenu, T., Chelly, J., 2006. Molecular genetics of Rett syndrome: when DNA methylation goes unrecognized. Nat. Rev. Genet. 7, 415–426.

Buchovecky, C.M., Turley, S.D., Brown, H.M., Kyle, S.M., McDonald, J.G., Liu, B., Pieper, A.A., Huang, W., Katz, D.M., Russell, D.W., Shendure, J., Justice, M.J., 2013. A suppressor screen in Mecp2 mutant mice implicates cholesterol metabolism in Rett syndrome. Nat. Genet. 45, 1013–1020.

Burford, B., Kerr, A.M., Macleod, H.A., 2003. Nurse recognition of early deviation in development in home videos of infants with Rett disorder. J. Intellect. Disabil. Res. 47, 588–596.

Calfa, G., Percy, A.K., Pozzo-Miller, L., 2011. Experimental models of Rett syndrome based on Mecp2 dysfunction. Exp. Biol. Med. (Maywood) 236, 3–19.

Chahrour, M., Zoghbi, H.Y., 2007. The story of Rett syndrome: from clinic to neurobiology. Neuron 56, 422–437.

Chahrour, M., Jung, S.Y., Shaw, C., Zhou, X., Wong, S.T., Qin, J., Zoghbi, H.Y., 2008. MeCP2, a key contributor to neurological disease, activates and represses transcription. Science 320, 1224–1229.

Chen, R.Z., Akbarian, S., Tudor, M., Jaenisch, R., 2001. Deficiency of methyl-CpG binding protein-2 in CNS neurons results in a Rett-like phenotype in mice. Nat. Genet. 27, 327–331.

Cheung, A.Y., Horvath, L.M., Grafodatskaya, D., Pasceri, P., Weksberg, R., Hotta, A., Carrel, L., Ellis, J., 2011. Isolation of MECP2-null Rett syndrome patient hiPS cells and isogenic controls through X-chromosome inactivation. Hum. Mol. Genet. 20, 2103–2115.

Ciccoli, L., Leoncini, S., Signorini, C., Comporti, M., 2008. Iron and erythrocytes: physiological and pathophysiological aspects. In: Valacchi, G., Davis, P. (Eds.), Oxidant in Biology: A Question of Balance. Springer, pp. 167–181.

Dani, V.S., Chang, Q., Maffei, A., Turrigiano, G.G., Jaenisch, R., Nelson, S.B., 2005. Reduced cortical activity due to a shift in the balance between excitation and inhibition in a mouse model of Rett syndrome. Proc. Natl. Acad. Sci. U. S. A. 102, 12560–12565.

De Felice, C., Ciccoli, L., Leoncini, S., Signorini, C., Rossi, M., Vannuccini, L., Guazzi, G., Latini, G., Comporti, M., Valacchi, G., Hayek, J., 2009. Systemic oxidative stress in classic Rett syndrome. Free Radic. Biol. Med. 47, 440–448.

De Felice, C., Guazzi, G., Rossi, M., Ciccoli, L., Signorini, C., Leoncini, S., Tonni, G., Latini, G., Valacchi, G., Hayek, J., 2010. Unrecognized lung disease in classic Rett syndrome: a physiologic and high-resolution CT imaging study. Chest 138, 386–392.

De Felice, C., Signorini, C., Durand, T., Oger, C., Guy, A., Bultel-Ponce, V., Galano, J.M., Ciccoli, L., Leoncini, S., D'Esposito, M., Filosa, S., Pecorelli, A., Valacchi, G., Hayek, J., 2011. F2-dihomo-isoprostanes as potential early biomarkers of lipid oxidative damage in Rett syndrome. J. Lipid Res. 52, 2287–2297.

De Felice, C., Signorini, C., Durand, T., Ciccoli, L., Leoncini, S., D'Esposito, M., Filosa, S., Oger, C., Guy, A., Bultel-Ponce, V., Galano, J.M., Pecorelli, A., De Felice, L., Valacchi, G., Hayek, J., 2012a. Partial rescue of Rett syndrome by omega-3 polyunsaturated fatty acids (PUFAs) oil. Genes Nutr. 7, 447–458.

De Felice, C., Signorini, C., Leoncini, S., Pecorelli, A., Durand, T., Valacchi, G., Ciccoli, L., Hayek, J., 2012b. The role of oxidative stress in Rett syndrome: an overview. Ann. N. Y. Acad. Sci. 1259, 121–135.

De Felice, C., Signorini, C., Leoncini, S., Pecorelli, A., Durand, T., Galano, J.M., Bultel-Poncé, V., Guy, A., Oger, C., Zollo, G., Valacchi, G., Ciccoli, L., Hayek, J., 2013. Fatty acids and autism spectrum disorders: the Rett syndrome conundrum. Food Nutr. Sci. 71–75.

De Felice, C., Rossi, M., Leoncini, S., Chisci, G., Signorini, C., Lonetti, G., Vannuccini, L., Spina, D., Ginori, A., Iacona, I., Cortelazzo, A., Pecorelli, A., Valacchi, G., Ciccoli, L., Pizzorusso, T., Hayek, J., 2014. Inflammatory lung disease in Rett syndrome. Mediat. Inflamm. 2014, 560120. http://dx.doi.org/10.1155/2014/560120.

De Filippis, B., Ricceri, L., Laviola, G., 2010. Early postnatal behavioral changes in the Mecp2-308 truncation mouse model of Rett syndrome. Genes Brain Behav. 9, 213–223.

Delepine, C., Nectoux, J., Bahi-Buisson, N., Chelly, J., Bienvenu, T., 2013. MeCP2 deficiency is associated with impaired microtubule stability. FEBS Lett. 587, 245–253.

Derecki, N.C., Cronk, J.C., Lu, Z., Xu, E., Abbott, S.B., Guyenet, P.G., Kipnis, J., 2012. Wild-type microglia arrest pathology in a mouse model of Rett syndrome. Nature 484, 105–109.

Derecki, N.C., Cronk, J.C., Kipnis, J., 2013. The role of microglia in brain maintenance: implications for Rett syndrome. Trends Immunol. 34, 144–150.

Durand, T., De Felice, C., Signorini, C., Oger, C., Bultel-Ponce, V., Guy, A., Galano, J.M., Leoncini, S., Ciccoli, L., Pecorelli, A., Valacchi, G., Hayek, J., 2013. F(2)-dihomo-isoprostanes and brain white matter damage in stage 1 Rett syndrome. Biochimie 95, 86–90.

Einspieler, C., Kerr, A.M., Prechtl, H.F., 2005a. Abnormal general movements in girls with Rett disorder: the first four months of life. Brain Dev. 27 (Suppl. 1), S8–S13.

Einspieler, C., Kerr, A.M., Prechtl, H.F., 2005b. Is the early development of girls with Rett disorder really normal? Pediatr. Res. 57, 696–700.

Ferguson, L.R., 2010. Chronic inflammation and mutagenesis. Mutat. Res. 690, 3–11.

Galano, J.M., Mas, E., Barden, A., Mori, T.A., Signorini, C., De Felice, C., Barrett, A., Opere, C., Pinot, E., Schwedhelm, E., Benndorf, R., Roy, J., Le Guennec, J.Y., Oger, C., Durand, T., 2013. Isoprostanes and neuroprostanes: total synthesis, biological activity and biomarkers of oxidative stress in humans. Prostaglandins Other Lipid Mediat. 107, 95–102.

Garg, S.K., Lioy, D.T., Cheval, H., McGann, J.C., Bissonnette, J.M., Murtha, M.J., Foust, K.D., Kaspar, B.K., Bird, A., Mandel, G., 2013. Systemic delivery of MeCP2 rescues behavioral and cellular deficits in female mouse models of Rett syndrome. J. Neurosci. 33, 13612–13620.

Goffin, D., Allen, M., Zhang, L., Amorim, M., Wang, I.T., Reyes, A.R., Mercado-Berton, A., Ong, C., Cohen, S., Hu, L., Blendy, J.A., Carlson, G.C., Siegel, S.J., Greenberg, M.E., Zhou, Z., 2012. Rett syndrome mutation MeCP2 T158A disrupts DNA binding, protein stability and ERP responses. Nat. Neurosci. 15, 274–283.

Grillo, E., Lo Rizzo, C., Bianciardi, L., Bizzarri, V., Baldassarri, M., Spiga, O., Furini, S., De Felice, C., Signorini, C., Leoncini, S., Pecorelli, A., Ciccoli, L., Mencarelli, M.A., Hayek, J., Meloni, I., Ariani, F., Mari, F., Renieri, A., 2013. Revealing the complexity of a monogenic disease: Rett syndrome exome sequencing. PLoS One 8, e56599.

Grosser, E., Hirt, U., Janc, O.A., Menzfeld, C., Fischer, M., Kempkes, B., Vogelgesang, S., Manzke, T.U., Opitz, L., Salinas-Riester, G., Muller, M., 2012. Oxidative burden and mitochondrial dysfunction in a mouse model of Rett syndrome. Neurobiol. Dis. 48, 102–114.

Guy, J., Hendrich, B., Holmes, M., Martin, J.E., Bird, A., 2001. A mouse Mecp2-null mutation causes neurological symptoms that mimic Rett syndrome. Nat. Genet. 27, 322–326.

Guy, J., Gan, J., Selfridge, J., Cobb, S., Bird, A., 2007. Reversal of neurological defects in a mouse model of Rett syndrome. Science 315, 1143–1147.

Guy, J., Cheval, H., Selfridge, J., Bird, A., 2011. The role of MeCP2 in the brain. Annu. Rev. Cell Dev. Biol. 27, 631–652.

Hagberg, B., 2002. Clinical manifestations and stages of Rett syndrome. Ment. Retard. Dev. Disabil. Res. Rev. 8, 61–65.

Halliwell, B., Gutteridge, J., 2007. Free Radicals in Biology and Medicine, Fourth edition. Oxford University Press.

Han, K., Gennarino, V.A., Lee, Y., Pang, K., Hashimoto-Torii, K., Choufani, S., Raju, C.S., Oldham, M.C., Weksberg, R., Rakic, P., Liu, Z., Zoghbi, H.Y., 2013. Human-specific regulation of MeCP2 levels in fetal brains by microRNA miR-483-5p. Genes Dev. 27, 485–490.

Janc, O.A., Muller, M., 2014. The free radical scavenger Trolox dampens neuronal hyperexcitability, reinstates synaptic plasticity, and improves hypoxia tolerance in a mouse model of Rett syndrome. Front. Cell. Neurosci. 8, 56.

Jones, P.L., Veenstra, G.J., Wade, P.A., Vermaak, D., Kass, S.U., Landsberger, N., Strouboulis, J., Wolffe, A.P., 1998. Methylated DNA and MeCP2 recruit histone deacetylase to repress transcription. Nat. Genet. 19, 187–191.

Katz, D.M., Berger-Sweeney, J.E., Eubanks, J.H., Justice, M.J., Neul, J.L., Pozzo-Miller, L., Blue, M.E., Christian, D., Crawley, J.N., Giustetto, M., Guy, J., Howell, C.J., Kron, M., Nelson, S. B., Samaco, R.C., Schaevitz, L.R., St Hillaire-Clarke, C., Young, J.L., Zoghbi, H.Y., Mamounas, L.A., 2012. Preclinical research in Rett syndrome: setting the foundation for translational success. Dis. Model Mech. 5, 733–745.

Leonard, H., Bower, C., 1998. Is the girl with Rett syndrome normal at birth? Dev. Med. Child Neurol. 40, 115–121.

Leoncini, S., De Felice, C., Signorini, C., Pecorelli, A., Durand, T., Valacchi, G., Ciccoli, L., Hayek, J., 2011. Oxidative stress in Rett syndrome: natural history, genotype, and variants. Redox Rep. 16, 145–153.

Lioy, D.T., Garg, S.K., Monaghan, C.E., Raber, J., Foust, K.D., Kaspar, B.K., Hirrlinger, P.G., Kirchhoff, F., Bissonnette, J.M., Ballas, N., Mandel, G., 2011. A role for glia in the progression of Rett's syndrome. Nature 475, 497–500.

Marschik, P.B., Lanator, I., Freilinger, M., Prechtl, H.F.R., Einspieler, C., 2011. Early signs and later neurophysiological correlates of Rett syndrome. Klin. Neurophysiol. 42, 22–26.

Moretti, P., Bouwknecht, J.A., Teague, R., Paylor, R., Zoghbi, H.Y., 2005. Abnormalities of social interactions and home-cage behavior in a mouse model of Rett syndrome. Hum. Mol. Genet. 14, 205–220.

Moretti, P., Levenson, J.M., Battaglia, F., Atkinson, R., Teague, R., Antalffy, B., Armstrong, D., Arancio, O., Sweatt, J.D., Zoghbi, H.Y., 2006. Learning and memory and synaptic plasticity are impaired in a mouse model of Rett syndrome. J. Neurosci. 26, 319–327.

Nagy, G., Ackerman, S.L., 2013. Cholesterol metabolism and Rett syndrome pathogenesis. Nat. Genet. 45, 965–967.

Neul, J.L., Kaufmann, W.E., Glaze, D.G., Christodoulou, J., Clarke, A.J., Bahi-Buisson, N., Leonard, H., Bailey, M.E., Schanen, N.C., Zappella, M., Renieri, A., Huppke, P., Percy, A.K., 2010. Rett syndrome: revised diagnostic criteria and nomenclature. Ann. Neurol. 68, 944–950.

Panayotis, N., Pratte, M., Borges-Correia, A., Ghata, A., Villard, L., Roux, J.C., 2011. Morphological and functional alterations in the substantia nigra pars compacta of the Mecp2-null mouse. Neurobiol. Dis. 41, 385–397.

Pecorelli, A., Ciccoli, L., Signorini, C., Leoncini, S., Giardini, A., D'Esposito, M., Filosa, S., Hayek, J., De Felice, C., Valacchi, G., 2011. Increased levels of 4HNE-protein plasma adducts in Rett syndrome. Clin. Biochem. 44, 368–371.

Pecorelli, A., Leoncini, S., De Felice, C., Signorini, C., Cerrone, C., Valacchi, G., Ciccoli, L., Hayek, J., 2013. Non-protein-bound iron and 4-hydroxynonenal protein adducts in classic autism. Brain Dev. 35, 146–154.

Picker, J.D., Yang, R., Ricceri, L., Berger-Sweeney, J., 2006. An altered neonatal behavioral phenotype in Mecp2 mutant mice. Neuroreport 17, 541–544.

Poli, G., Schaur, R.J., Siems, W.G., Leonarduzzi, G., 2008. 4-Hydroxynonenal: a membrane lipid oxidation product of medicinal interest. Med. Res. Rev. 28, 569–631.

Praticò, D., 2010. The neurobiology of isoprostanes and Alzheimer's disease. Biochim. Biophys. Acta 1801, 930–933.

Ramirez, J.M., Ward, C.S., Neul, J.L., 2013. Breathing challenges in Rett syndrome: lessons learned from humans and animal models. Respir. Physiol. Neurobiol. 189, 280–287.

Rett, A., 1966. On a unusual brain atrophy syndrome in hyperammonemia in childhood. Wien. Med. Wochenschr. 116, 723–726.

Ricceri, L., De Filippis, B., Laviola, G., 2008. Mouse models of Rett syndrome: from behavioural phenotyping to preclinical evaluation of new therapeutic approaches. Behav. Pharmacol. 19, 501–517.

Robinson, L., Guy, J., McKay, L., Brockett, E., Spike, R.C., Selfridge, J., De Sousa, D., Merusi, C., Riedel, G., Bird, A., Cobb, S.R., 2012. Morphological and functional reversal of phenotypes in a mouse model of Rett syndrome. Brain 135, 2699–2710.

Rouault, T.A., 2013. Iron metabolism in the CNS: implications for neurodegenerative diseases. Nat. Rev. Neurosci. 14, 551–564.

Santos, M., Silva-Fernandes, A., Oliveira, P., Sousa, N., Maciel, P., 2007. Evidence for abnormal early development in a mouse model of Rett syndrome. Genes Brain Behav. 6, 277–286.

Schroder, N., Figueiredo, L.S., de Lima, M.N., 2013. Role of brain iron accumulation in cognitive dysfunction: evidence from animal models and human studies. J. Alzheimer's Dis. 34, 797–812.

Shahbazian, M., Young, J., Yuva-Paylor, L., Spencer, C., Antalffy, B., Noebels, J., Armstrong, D., Paylor, R., Zoghbi, H., 2002. Mice with truncated MeCP2 recapitulate many Rett syndrome features and display hyperacetylation of histone H3. Neuron 35, 243–254.

Sierra, C., Vilaseca, M.A., Brandi, N., Artuch, R., Mira, A., Nieto, M., Pineda, M., 2001. Oxidative stress in Rett syndrome. Brain Dev. 23 (Suppl. 1), S236–S239.

Signorini, C., Comporti, M., Giorgi, G., 2003. Ion trap tandem mass spectrometric determination of F2-isoprostanes. J. Mass Spectrom. 38, 1067–1074.

Signorini, C., Ciccoli, L., Leoncini, S., Carloni, S., Perrone, S., Comporti, M., Balduini, W., Buonocore, G., 2009. Free iron, total F-isoprostanes and total F-neuroprostanes in a model of neonatal hypoxic–ischemic encephalopathy: neuroprotective effect of melatonin. J. Pineal Res. 46, 148–154.

Signorini, C., De Felice, C., Leoncini, S., Giardini, A., D'Esposito, M., Filosa, S., Della Ragione, F., Rossi, M., Pecorelli, A., Valacchi, G., Ciccoli, L., Hayek, J., 2011. F(4)-neuroprostanes mediate neurological severity in Rett syndrome. Clin. Chim. Acta 412, 1399–1406.

Signorini, C., De Felice, C., Durand, T., Oger, C., Galano, J.M., Leoncini, S., Pecorelli, A., Valacchi, G., Ciccoli, L., Hayek, J., 2013. Isoprostanes and 4-hydroxy-2-nonenal: markers or mediators of disease? Focus on Rett syndrome as a model of autism spectrum disorder. Oxid. Med. Cell. Longev. 2013, 343824.

Singh, M., Dang, T.N., Arseneault, M., Ramassamy, C., 2010. Role of by-products of lipid oxidation in Alzheimer's disease brain: a focus on acrolein. J. Alzheimer's Dis. 21, 741–756.

Sticozzi, C., Belmonte, G., Pecorelli, A., Cervellati, F., Leoncini, S., Signorini, C., Ciccoli, L., De Felice, C., Hayek, J., Valacchi, G., 2013. Scavenger receptor B1 post-translational modifications in Rett syndrome. FEBS Lett. 587, 2199–2204.

Temudo, T., Maciel, P., Sequeiros, J., 2007. Abnormal movements in Rett syndrome are present before the regression period: a case study. Mov. Disord. 22, 2284–2287.

Tronche, F., Kellendonk, C., Kretz, O., Gass, P., Anlag, K., Orban, P.C., Bock, R., Klein, R., Schutz, G., 1999. Disruption of the glucocorticoid receptor gene in the nervous system results in reduced anxiety. Nat. Genet. 23, 99–103.

Valacchi, G., Pecorelli, A., Signorini, C., Leoncini, S., Ciccoli, L., De Felice, C., Hayek, J., 2014. 4HNE protein adducts in autistic spectrum disorders: Rett syndrome and autism. In: Patel, V.B., P.V.R., Martin, C.R. (Eds.), Comprehensive Guide to Autism. Springer, New York, pp. 2667–2688.

Weaving, L.S., Ellaway, C.J., Gecz, J., Christodoulou, J., 2005. Rett syndrome: clinical review and genetic update. J. Med. Genet. 42, 1–7.

Yazdani, M., Deogracias, R., Guy, J., Poot, R.A., Bird, A., Barde, Y.A., 2012. Disease modeling using embryonic stem cells: MeCP2 regulates nuclear size and RNA synthesis in neurons. Stem Cells 30, 2128–2139.

Zachariah, R.M., Olson, C.O., Ezeonwuka, C., Rastegar, M., 2012. Novel MeCP2 isoform-specific antibody reveals the endogenous MeCP2E1 expression in murine brain, primary neurons and astrocytes. PLoS One 7, e49763.